Proceedings of the 2022 Design of Medical Devices Conference
DMD2022
April 11-14, 2022, Minneapolis, MN, USA

DMD2022-1026

FULLY UNTETHERED AND STRETCHABLE WEARABLE ELECTRONIC BANDAGE FOR MEASURING KNEE MOTION

Matthew McManigal
Wellsandt Lab
College of Allied Health Professions
University of Nebraska Medical Center
Omaha, NE

Renick Wilson
Smart Materials and Robotics Laboratory
Department of Mechanical & Materials Engineering
University of Nebraska-Lincoln
Lincoln, NE

Patrick McManigal
Smart Materials and Robotics Laboratory
Department of Mechanical & Materials Engineering
University of Nebraska-Lincoln
Lincoln, NE

Brooke Beran
Wellsandt Lab
Division of Physical Therapy Education
University of Nebraska Medical Center
Omaha, NE

Dr. Elizabeth Wellsandt
Wellsandt Lab
Division of Physical Therapy Education
University of Nebraska Medical Center
Omaha, NE

Dr. Eric J. Markvicka
Smart Materials and Robotics Laboratory
Department of Mechanical & Materials Engineering
University of Nebraska-Lincoln
Lincoln, NE

ABSTRACT

Wearable electronics capable of measuring three-dimensional knee joint angle would provide new methods to predict both anterior cruciate ligament (ACL) injuries and the risk of developing early knee osteoarthritis. However, knee joint angle assessment is currently limited, due to the lack of validated wearable and untethered technologies that can be deployed in natural environments and rural or community settings. To address this challenge, we created a fully untethered, wearable electronic device to continuously measure knee joint angle using two inertial measurement unit (IMU) sensors. The wearable device is composed of a stretchable circuit assembled on a spandex-blend fabric substrate that allows the device to conform to the knee without restricting natural human movement. The fabric substrate allows the electronic circuit to be reused, while increasing the robustness of the device. Finally, we demonstrate the ability of the device to continuously measure sagittal plane knee joint angle during natural human movements outside of a laboratory environment.

Keywords: wearable electronics, joint angles, inertial measurement units

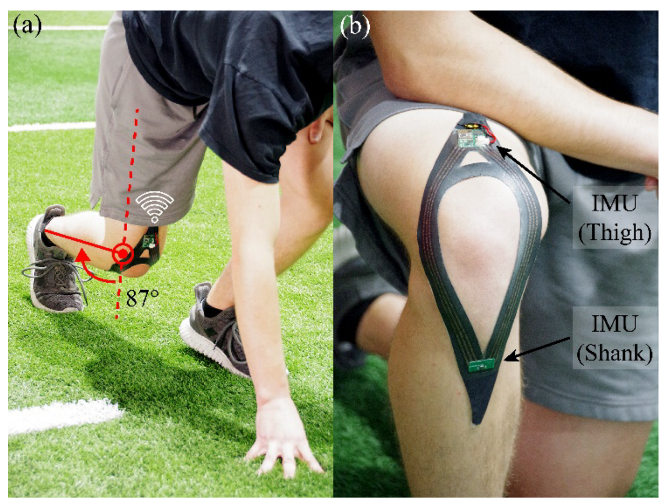

FIGURE 1: (a) THE FULLY UNTETHERED AND STRETCHABLE, WEARABLE ELECTRONIC BANDAGE IS IS SHOWN ATTACHED TO THE KNEE FOR MEASURING KNEE MOTION. **(b)** THE WEARABLE DEVICE CONTAINS AN INERTIAL MEASURMENT UNIT (IMU) LOCATED ON THE THIGH AND SHANK. DURING OPERATION, MOTION DATA IS COLLECTED FROM EACH SENSOR, THE DATA IS WIRELESSLY TRANSMITTED TO A NEARBY COMPUTER, AND JOINT ANGLE IS ESTIMATED.

© 2022 by ASME

1. INTRODUCTION

Knee injuries account for one-third of all severe orthopedic injuries sustained during sports and recreational activities and can have lasting consequences [1]. Unfortunately, outcomes after major knee injuries are frequently poor; for example, following reconstruction of an ACL injury, only 55% of athletes return to participating in competitive sports [2]. Moreover, 50% of teenagers and young adults will develop early knee osteoarthritis within 10 years of an ACL or meniscus tear [3, 4]. It has been found that kinematic parameters, such as knee flexion and adduction angles, can predict ACL injuries, probability of returning to sport activities, and risk for developing early knee osteoarthritis [5-7]. Fortunately, an estimated 50% of ACL injuries can be prevented via injury prevention programs [8]. Typically, kinematic variables are quantified in motion capture laboratories. However, due to high equipment costs and physical space requirements, these laboratories are uncommon in clinical and public settings. Additionally, typical laboratory settings make it difficult to analyze movement patterns as they would occur in a natural environment (e.g., soccer field, basketball court, running track, etc.). Despite strong evidence that movement patterns can predict both knee injuries and outcomes following injury, assessments are unavailable in clinical and community settings due to the lack of mobile technologies that have been validated to measure biomechanical parameters at the knee joint.

Current methods of measuring knee joint-angles during dynamic movements include motion capture camera systems and IMUs [9-11]. Motion capture camera systems are very costly and difficult to setup, so these systems are typically found only in laboratory settings. While many joint-angle algorithms have been developed for IMUs, commercially available IMU systems used in research and the film-industry are prohibitively expensive for widespread use. Several commercially available wearable electronics are increasingly widespread. However, these products are only capable of tracking activity or step count. Recent advancements in stretchable electronics offer new opportunities to create functional electronic devices that mimic the mechanical properties of natural human skin [12].

Here, we introduce a fully untethered and stretchable, wearable electronic bandage for measuring knee joint angle. To enable use outside of a laboratory environment, all the necessary electronic components for sensing, signal processing, and wireless communication are tightly integrated. The wearable electronic bandage was demonstrated to measure sagittal plane knee angle during gait within known anatomical limits of knee flexion and extension.

2. MATERIALS AND METHODS

The wearable device for measuring knee joint angle is composed of a multiuse stretchable electronic circuit and replaceable skin adhesive (**FIGURE 2**). The multiuse stretchable electronic circuit is composed of two printed circuit boards (PCBs) that are wired together using six copper traces (**FIGURE 2a**). The two PCBs contain the electronic components required for joint-angle data collection and include two IMUs

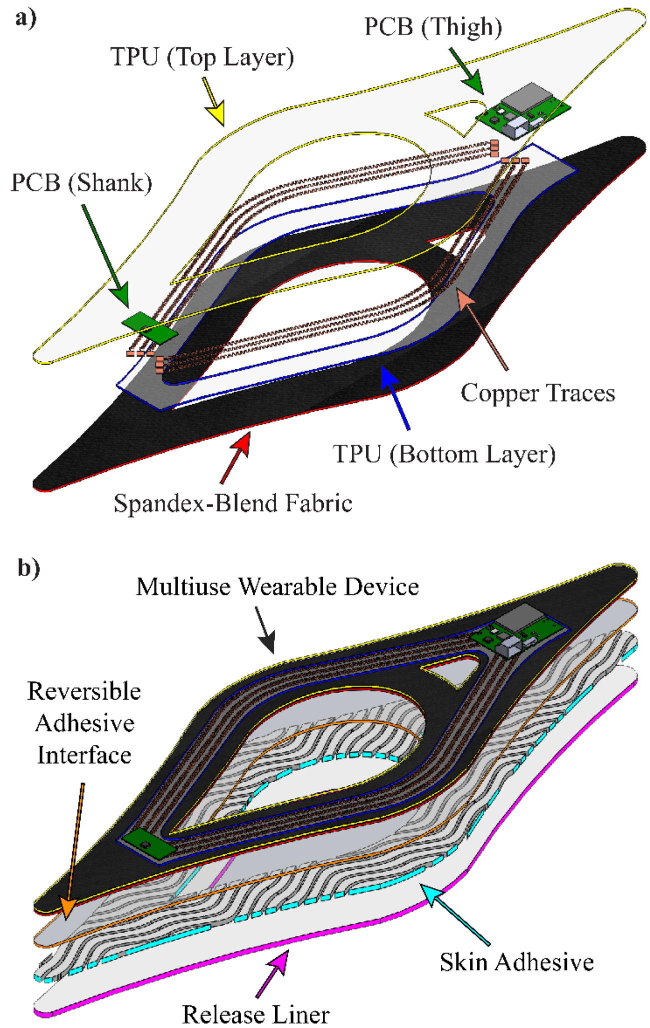

FIGURE 2: (a) EXPLODED VIEW OF THE MULTIUSE WEARABLE DEVICE FOR MEASURING JOINT-LEVEL HUMAN MOTION OF THE KNEE. **(b)** EXPLODED VIEW OF THE REPLACEABLE SKIN ADHESIVE THAT CAN REVERSIBLY ATTACH TO THE WEARABLE DEVICE UTILIZING A REVERSIBLE ADHESIVE INTERFACE.

(ICM20948, InvenSense), a microcontroller (ATMega328p, Microchip), a 2.4GHz wireless transceiver (nRF24L01+, Nordic Semiconductor), power regulation, and a rechargeable Li-Ion battery (3.7v, 500mAh) for up to 2 hours of continuous data collection. Each IMU sensor contains a three-axis accelerometer, gyroscope, and magnetometer to track human motion. The PCBs are electrically connected using deterministically patterned copper traces, enabling the copper traces to deform during joint movement. The circuit is bonded to the fabric substrate with a thermoplastic polyurethane (TPU) heat-sensitive film (2mil 3412, Bemis). Finally, a second sheet of TPU is vacuum formed over the top of the PCBs and copper traces for additional protection. A replaceable skin adhesive is attached to the bottom side of the fabric substrate for attachment to the skin (**FIGURE**

© 2022 by ASME

2b). The replaceable skin adhesive is composed of a reversible adhesive interface (Tegaderm, 3M), a soft skin adhesive (Silbione RT Gel 4717), and a polytetrafluoroethylene (PTFE) release liner. The symmetric device design allows use on the right and left knee. Cutouts have been introduced to allow the device to conform around the patella.

2.1 Fabrication of the Multiuse Wearable Device

The multiuse wearable device was fabricated using a combination of material patterning using laser cutting and computer-controlled cutting machines. The individual layers were laminated together using heat sensitive films. First, the spandex-blend fabric and bottom TPU layer were cut to shape using a computer-controlled cutting machine (Maker, Cricut). The fabric and TPU layer were then bonded together in a heat press at 150°C for 25 seconds. Next, the serpentine patterned copper traces were laser patterned from a flexible copper clad sheet (FR7031, DuPont) using a UV laser micromachining system (Protolaser U4, LPKF) at a power of 2 W at 135 mm sec^{-1} with 18 repetitions [13]. The film was patterned on a silicone sheet (Sylgard 184, Dow Corning with oligomer-to-curing agent ratio of 25:1). After patterning, the copper film was cleaned using isopropyl alcohol, and the excess was removed. The copper traces were then aligned and bonded to the TPU layer on the fabric using a heat press at 150°C for 25 seconds.

Next, the PCBs were attached to the copper traces. The PCBs were bonded to the terminals of the copper traces using an anisotropic conductive file (ACF; ECATT 9703, 3M). The ACF was first bonded to the underside of the PCBs in a heat press at 163°C for 10 seconds. The PCBs were then bonded to the copper traces in a heat press at 163°C for 15 seconds. After the 15 second heating period, the heat press was turned off and the samples were left in the press until the heat press returned to room temperature. The ACF provides an electrical and mechanical interface. The PCBs were then secured to the TPU layer in a heat press at 150°C for 25 seconds.

Finally, using a vacuum former, a layer of TPU was heated and vacuum formed to the top of the device. Excess material was then trimmed from the top TPU layer. The top TPU layer provides increased robustness and durability to the stretchable electronic circuit.

2.2 Fabrication of the Replaceable Adhesive

The replaceable skin adhesive allows the electronic circuit to directly adhere to the skin while allowing the electronic circuit to be reused. The skin adhesive is disposable and can be replaced as needed. The replaceable adhesive design is composed of three layers. The first layer is a reversible adhesive interface (Tegaderm, 3M), that adheres sufficiently to the fabric substrate such that it does not delaminate during intense activity, yet it can still be easily peeled from the fabric. The second layer is a soft, elastomeric skin adhesive (Silbione RT Gel 4717) that directly attaches to the skin. The skin adhesive is a two-component silicone elastomer that can be cured at room temperature. The skin adhesive is patterned in a serpentine pattern to allow sweat to drain during exercise. The final layer is a 0.005”-thick sheet of PTFE that functions as a release liner for the skin adhesive, which is removed before application of the device.

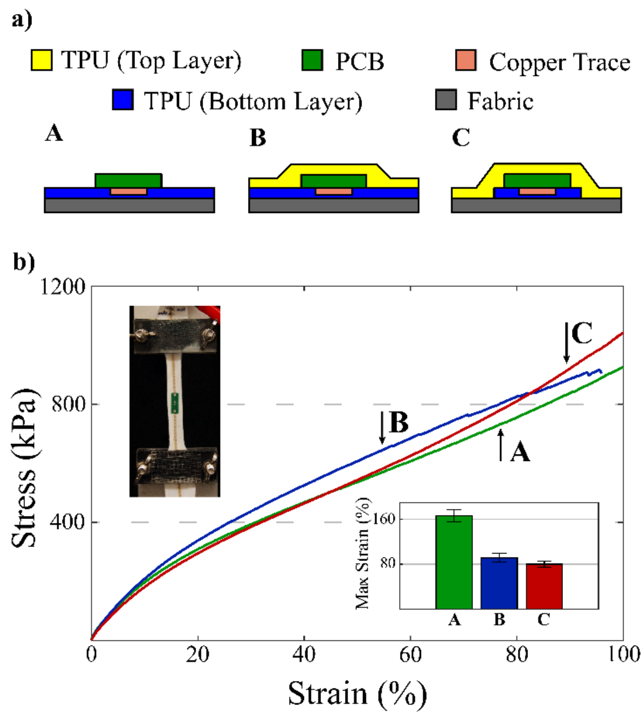

FIGURE 3: **(a)** CROSS-SECTIONAL ILLUSTRATIONS OF THE DIFFERENT CONFIGURATIONS (A, B, C) OF THE ELECTRONIC BANDAGE. **(b)** MEAN STRESS VERSUS STRAIN UNDER UNIAXIAL DEFORMATION OF THE 3 DIFFERENT CONFIGURATIONS (A, B, C) SHOWN IN 3(a) **(LEFT INSET)** PHOTOGRAPH OF DOG-BONE SAMPLE DURING UNIAXIAL DEFORMATION TESTING **(RIGHT INSET)** ELECTRICAL FAILURE STRAIN FOR THE DIFFERENT CONFIGURATIONS SHOWN IN 3(a).

The skin adhesive was applied to the non-adhesive side of the reversible adhesive. Stencil lithography was used to pattern the skin adhesive in a serpentine pattern using a thin-film applicator. The mask was then removed, and the skin adhesive was cured at 80°C for 10 minutes. After curing, the release liner was placed over the skin adhesive. Finally, the replaceable adhesive was cut into the desired shape using a CO_2-laser cutter (Mini 24, Epilog).

2.3 Mechanical Characterization

The stretchable electronic circuit was characterized under tensile loading to evaluate the material performance. A PCB with two electrical interconnects and a zero-ohm resistor was laminated onto a fabric substrate using three different combinations of TPU films and layering (**FIGURE 3a**). The TPU pattern for group A consisted of a single layer of TPU between the fabric and electrical circuit. Group B was fabricated like group A, but with an additional TPU layer vacuum formed over the top of the entire device. Group C featured the same fabrication as group B; however, the width of the bottom TPU layer was reduced to closely match the profile of the copper

© 2022 by ASME

traces and PCB. Each dog-bone sample included two copper traces that ran from the PCB to the end of the sample (**FIGURE 3b LEFT INSET**). The different configurations were characterized with a material testing machine (5966, Instron) at a loading rate of 100 mm min^{-1}, using a dog-bone geometry (ASTM D412A). The stress versus strain up to 100% strain or until electrical failure occurred is shown in **FIGURE 3b**. During testing the electrical resistance was measured using a digital multimeter. In all configurations, the copper trace electrically failed before mechanical failure occurred. The electrical failure strain is shown in **FIGURE 3b RIGHT INSET**.

2.4 Joint-Angle Algorithm

During use, the wearable device was placed on the anterior aspect of the knee, such that one IMU was arbitrarily placed on the distal, anterior thigh, and the other was arbitrarily placed on the proximal, anterior tibia. During operation, motion data, from the gyroscope and accelerometer, was wirelessly transmitted to a local computer from each IMU at a frequency of 120 Hz. To identify the approximate orientation of the sensors relative to the anatomical axes without physical measurements, a calibration procedure was first performed through three static poses, such that acceleration due to gravity was aligned with a unique anatomical axis in each pose. Joint angle was estimated utilizing strap-down gyroscope integration. Sensor orientation and joint angle were estimated following data collection using a custom MATLAB script.

3. RESULTS AND DISCUSSION

In all presented configurations, the wearable device was observed to be soft and highly deformable (E < 2.1 MPa) as shown in **FIGURE 3b**. All devices exceeded the maximum anticipated strain of 45% during physiological flexion and extension of a human knee joint [14]. While group A achieved the highest strain before electrical failure, the copper traces were observed to begin delaminating from the fabric substrate at 50% strain, and the traces completed delamination from the fabric substrate at electrical failure. If the copper traces delaminate from the fabric, there is a high risk of snagging and separating the trace from the PCBs that would ultimately cause electrical failure. The copper traces in groups B and C did not experience delamination from the fabric during testing, likely because the copper traces in these groups were sealed between two layers of TPU. The top TPU layer also improved robustness and durability of the wearable device. Group C was chosen for the multiuse wearable device design shown in **FIGURE 1**.

Finally, the wearable device was demonstrated outside of a laboratory environment to continuously measure sagittal-plane knee joint angle during walking. During the data collection, the sensor data was recorded on a nearby computer and post processed. As shown in **FIGURE 4**, the measured knee joint angle was shown to be similar to the characteristic pattern of a healthy participant [15]. This demonstration provided initial face validity to estimate knee joint angle within the expected range. Initial usability feedback indicated that the device was

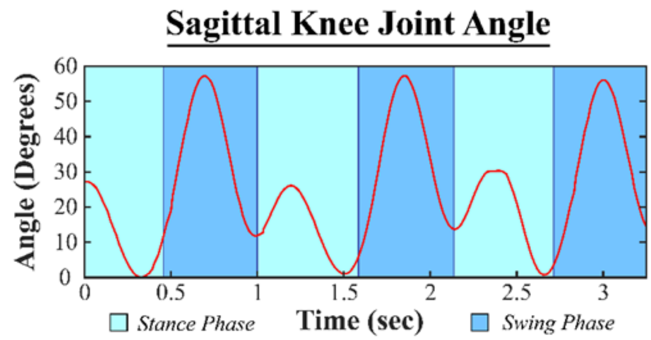

FIGURE 4: ESTIMATION OF SAGITTAL KNEE JOINT ANGLE DATA DURING GAIT.

comfortable, stayed in place during an active period of movement for up to one hour, and did not hinder knee motion; however, more feedback will be required to statistically evaluate the device's performance and wearability.

4. CONCLUSION

We have created a reusable, wearable device that can wirelessly collect human motion data and estimate knee joint angle outside of a laboratory environment. Future work will include optimization of the wearable device through observational human studies and validation of the knee joint angle algorithm against a 3D-motion capture system, the current gold-standard for measuring knee joint angles.

ACKNOWLEDGEMENTS

The authors acknowledge support from the Nebraska Research Initiative and Nebraska Tobacco Settlement Biomedical Research Development. Materials were fabricated and characterized using equipment that was purchased using funds from the Nebraska Tobacco Settlement Biomedical Research Development.

REFERENCES

[1] Kay, M.C., et al., *J Athl Train*, 2017. **52**(2): p. 117-128.
[2] Ardern, C.L., et al., *Br J Sports Med*, 2014. **48**(21): p. 1543-52.
[3] Lohmander, L.S., et al., *Am J Sports Med*, 2007. **35**(10): p. 1756-69.
[4] Oiestad, B.E., et al., *Am J Sports Med*, 2010. **38**(11): p. 2201-10.
[5] Wellsandt, E., et al., *Am J Sports Med*, 2016. **44**(1): p. 143-51.
[6] Paterno, M.V., et al., *Am J Sports Med*, 2010. **38**(10): p. 1968-78.
[7] Di Stasi, S.L., et al., *Am J Sports Med*, 2013. **41**(6): p. 1310-8.
[8] Donnell-Fink, L.A., et al., *PLoS One*, 2015. **10**(12): p. e0144063.
[9] Winter, D.A., Biomechanics and Motor Control of Human Movement, 1990.

© 2022 by ASME

[10] Seel, T., et al., *Sensors (Basel, Switzerland)*, 2014. **14**(4): p. 6891-6909.
[11] Seel, T., et al., *IFAC-PapersOnLine*, 2017. **50**(1): p. 8798-8803.
[12] Markvicka, E., et al., *Proceedings of the 2019 CHI Conference on Human Factors in Computing Systems.*, 2019. P. 1-10
[13] Markvicka, E., et al., *Advanced Functional Materials*., 2016 26.46, p. 8496-8504.
[14] Wessendorf, A. M., et al., *IEEE Transactions on Biomedical Engineering*, 2012. **59**(12), p. 3432-3438.
[15] Whittle, M.W., Gait analysis: an introduction, 1991.

 © 2022 by ASME